Int. J. Electrochem. Sci., 12 **(2017)** 9697 – 9713, doi: 10.20964/2017.10.28

International Journal of
ELECTROCHEMICAL
SCIENCE
www.electrochemsci.org

An investigation of the NO_3^- concentration effect on lead anodic electrochemical behavior in NaOH solution

Yunlong He[1], *Ruidong Xu*[1,2,*], *Shiwei He*[1], *Hansen Chen*[1], *Kuo Li*[1], *Yun Zhu*[1],
Qingfeng Shen[1]

[1] Faculty of Metallurgical and Energy Engineering, Kunming University of Science and Technology, Kunming 650093, China;
[2] State Key Laboratory of Complex Nonferrous Metal Resources Clean Utilization, Kunming 650093, China
[*]E-mail: rdxupaper@aliyun.com

Received: 25 June 2017 / *Accepted:* 4 August 2017 / *Published:* 12 September 2017

An electrochemical investigation of the effect of NO_3^- concentration on lead anodic behavior in 4 M NaOH solution was performed using cyclic voltammetry (CV) and electrochemical impedance spectroscopy (EIS). The results reveal that the NO_3^- concentration has a positive influence on the formation of PbO at -0.46 V (SHE) from 0.0～0.24 M and a negative influence from 0.36～0.60 M. A large dosage of NO_3^- benefits the formation of PbO_2. Mechanisms for NO_3^- influence on the formation of PbO and PbO_2 on the lead surface were proposed. The anodic electrochemical behavior of lead in NaOH-$NaNO_3$ solution was successfully illustrated based on the mechanisms. SEM observation provided surface morphologies of lead electrodes obtained after potentiostatic polarization at a fixed potential in NaOH solution with different NO_3^- concentrations. XPS results indicate that the lead electrode surface is composed of PbO, Pb_3O_4 and PbO_2, which agrees with the analysis results of the cyclic voltammogram.

Keywords: lead; anodic electrochemical behavior; cyclic voltammetry; sodium nitrate;

1. INTRODUCTION

The electrochemical behavior of lead in various aqueous media has attracted considerable attention from many investigators due to the instructive role of lead application in different areas, such as lead acid batteries, industrial hydrometallurgical processes, lead-silver alloys, etc. [1-7]. The electrochemical behavior of lead in acidic H_2SO_4 solution [8], neutral Na_2SO_4 solution[9], Na_2HPO_4 solution [10] and Na_2CO_3 solution[11] have been studied extensively to better understand the nature and mechanisms of lead in these aqueous media.

As another research focus, lead electrochemical behavior in alkali electrolytes was also investigated. It is reported that the corrosion behavior of lead in NaOH solution is related to the formation and chemical dissolution of PbO on lead surfaces [12]. Soluble Pb^{2+} or $HPbO_2^-$ can be generated at low applied current densities on lead surfaces, whereas PbO_2 film can be produced at higher current densities. However, at a constant current density condition both PbO and PbO_2 films can be obtained. In this system PbO was confirmed to be the primary film.

For further investigation, NO_3^- was dissolved in different electrolyte solutions in order to investigate its effect on the electrochemical behavior of lead. $NaNO_3$ added to Na_2CO_3 solutions can be considered as a pitting corrosion agent, such that the breakdown potential decreases and more pitting corrosion can be observed with the increase of nitrate concentration [12]. To investigate the passivation behavior of lead in NaOH solutions, a low concentration of NO_3^- was added to 0.1 M NaOH solution. It was found that nitrate ions are apt to stimulate the active dissolution of lead and tend to break down the passivation layer in NaOH solution [13]. In neutral $NaNO_3$ and NH_4NO_3 solution, dissolution experiments of metallic lead plates were performed using the rotating disk method [14]. The investigators concluded that the dissolution rate of lead increases with the increase of NO_3^- concentration.

Although previous studies have provided information about the electrochemical behavior of lead in low NaOH concentration solution, study of lead electrochemical behavior in highly concentrated NaOH solution with added NO_3^- is attractive because the literature in this area is very scarce.

The objective of the present investigation is to systematically study the effect of NO_3^- on lead electrochemical behavior in 4 M NaOH solution. Cyclic voltammetry (CV) and electrochemical impedance spectroscopy (EIS) were used to evaluate the influence of NO_3^- on lead electrochemical behavior. The composition and surface microstructures on a lead surface were determined by X-ray photoelectron spectroscopy (XPS) and scanning electron microscopy (SEM), respectively. These research results are helpful for providing the theoretical basis and technical support for either anticorrosion or oxidation leaching of lead in strong alkaline solutions with NO_3^- as an oxidizing agent.

2. EXPERIMENTAL

Cyclic voltammetry experiments on lead electrode were performed in a three-electrode system in 4 M NaOH solution with different concentrations of NO_3^- using an electrochemical working station (PARSTAT2273). The reference electrode was a saturated KCL standard electrode. All potentials in this work are presented vs SHE. An inert graphite electrode was employed as the counter electrode. The working electrode was a pure lead sheet (>99.99%) that was cut into 1 cm (length) ×1 cm (width) ×2 mm (thickness), then ground sequentially with 600 to 2000 grit SiC paper, rinsed with anhydrous ethanol (AR), and then washed with doubly distilled water. The reference electrode and working electrode were linked by a Luggin capillary filled with agar and potassium chloride. The distance between the reference electrode and working electrode was approximately equal to four times the capillary diameter. EIS experiments were performed at the same device at different potentials and NO_3^-

concentrations. Potential values used in EIS experiments were obtained from the cyclic voltammetry curves under different conditions. The chemical composition and microstructure of lead sheets (working electrode) were characterized by XPS and SEM.

High purity nitrogen gas was purged into the solutions for 15 minutes before every experiment. All experiments were conducted at ambient temperature (~25℃). The concentration of NaOH was controlled at 4 M, the NO_3^- concentration changed from 0.00 M to 0.60 M and the apparent exposed area of the working electrode was approximately 1 cm^2 during all experiments. Unnecessary areas were carefully sealed by insulation paste. All solutions were freshly prepared from analytical grade chemical reagents using doubly distilled water for each run.

3. THERMODYNAMIC EVALUATION FOR NO_3^- REDUCTION BY Pb USING φ-pH DIAGRAM

Many researchers have found that metals such as lead and iron can be applied as a reductant in nitrate solutions for the decomposition of nitrate ions [16-17]. Although previous studies confirm that NO_3^- in $NaNO_3$ solution can be reduced to NO_2^- by lead, a φ-pH diagram of the Pb-N-Na-H_2O system was constructed to better understand the thermodynamic behavior of Pb and NO_3^- [16,18]. A φ-pH diagram of the Pb-N-Na-H_2O system has been constructed in Fig. 1

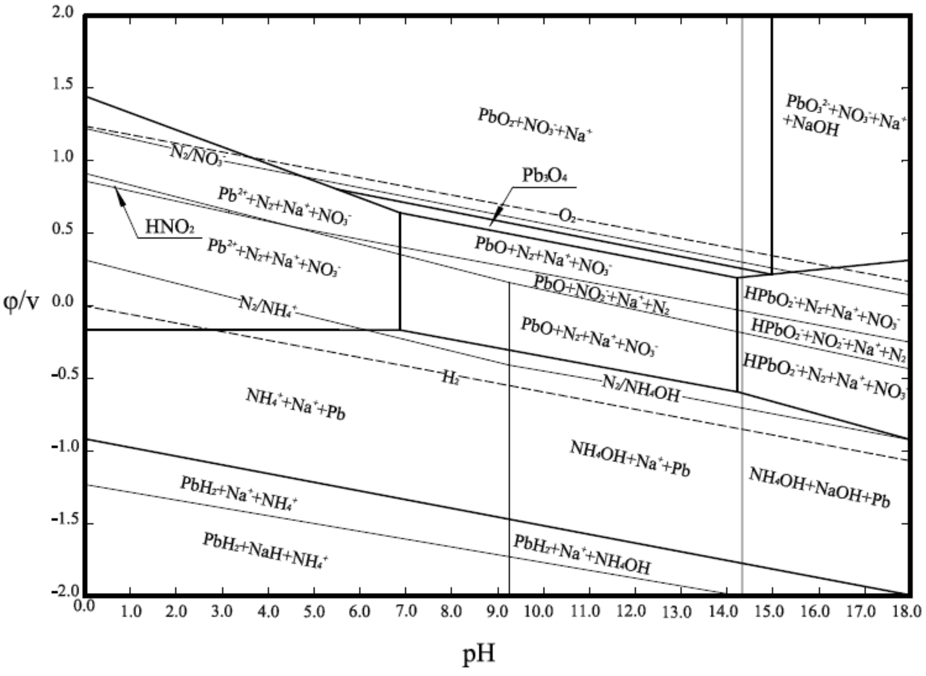

Figure 1. φ-pH diagram of the Pb-N-Na-H_2O system at 298 K, a_{Pb}=0.1 a_N=0.1; P_{N2}=1 atm; P_{O2}=1 atm; P_{H2}=1 atm.

Fig. 1 shows that metallic lead is thermodynamically stable in neutral solution without oxidation agents, but when oxidation agent is present in the solution, lead can be oxidized into PbO and then dissolve as Pb^{2+} in slightly alkaline solution or as $HPbO_2^-$ in very alkaline solution. When Pb or Pb^{2+} contact with a strong oxidation agent or high potential, PbO, Pb_3O_4 or even PbO_2 can be obtained (Pb_3O_4 is an intermediate oxide between PbO and PbO_2). PbO and PbO_2 are insoluble in neutral and moderately alkaline solution but they will dissolve as $HPbO_2^-$ and PbO_3^{2-}, respectively, in strongly alkaline solution [18].

Fig. 1 shows that the redox potential couple of PbO/Pb is much lower than that of NO_3^-/NO_2^-in a high pH region of the φ-pH diagram of the Pb-N-Na-H_2O system. These data predict that NO_3^- can be reduced to NO_2^- by lead in NaOH solution [16].

A series of redox reactions between $NO_3^-$and Pb in the Pb-N-Na-H_2O system are listed as follows:

$NO_3^- + Pb = NO_2^- + PbO$ (1)

$NO_2^- + 3Pb + H_2O = NH_3 + 3PbO + OH^-$ (2)

$NO_2^- + NH_3 = N_2 + H_2O + OH^-$ (3)

In the present investigation, the concentration of NaOH was controlled at 4 M, and the NO_3^- concentration changed from 0.00 M to 0.60 M, therefore a large amount of OH^- is present in the solution throughout the experiments. According to equation (2) and (3), a moderately or strongly alkaline solution is unfavorable to the reduction of NO_2^- because a large amount of OH^- may inhibit the decomposition of NO_2^-. Therefore, from a thermodynamic point of view, a conclusion can be drawn that NO_3^-can be reduced to NO_2^- by lead in NaOH-$NaNO_3$ solution at 298 K and $NO_2^-$is the main reduction product; metallic lead can be oxidized to oxides and dissolve as soluble lead species.

4. RESULTS AND DISCUSSION

4.1 Cyclic voltammetry study

4.1.1 Cyclic voltammetry curve

Cyclic voltammograms measured in 4 M NaOH solution with different NO_3^- concentrations are shown in Fig. 2. The NO_3^- concentration changed from 0.00 M to 0.60 M.

Three well defined peaks, A_I, A_{II} and A_{III}, were exhibited prior to the oxygen evolution potential in the anodic branch of the cyclic voltammograms shown in Fig. 2. Four cathodic peaks defined as C_I–C_{IV} prior to the hydrogen evolution potential were exhibited in the cathodic branch of the cyclic voltammograms.

The first anodic peak, A_I, appearing at -0.46 V, can be ascribed to the formation of PbO. At the beginning of the PbO formation process, a large amount of OH^- ions are adsorbed on the surface of the lead electrode in alkaline solution, and the main reactions can be listed as follows [19]:

$Pb + OH^- = PbOH_{ads} + e^-$ (4)

$PbOH_{ads} + OH^- = Pb(OH)_2 + e^-$ (5)

Most of the $Pb(OH)_2$ formed on the surface of the lead electrode will quickly dissolve in the form of $Pb(OH)_3^-$. However, the residuary $Pb(OH)_2$ will dehydrate and transform into PbO on the surface of the lead electrode [19]. To exhibit the anodic electrochemical reactions more clearly, the mechanism scheme of the elementary reactions on the surface of the lead electrode in NaOH solution without NO_3^- was proposed in Fig. 3 [8,19].

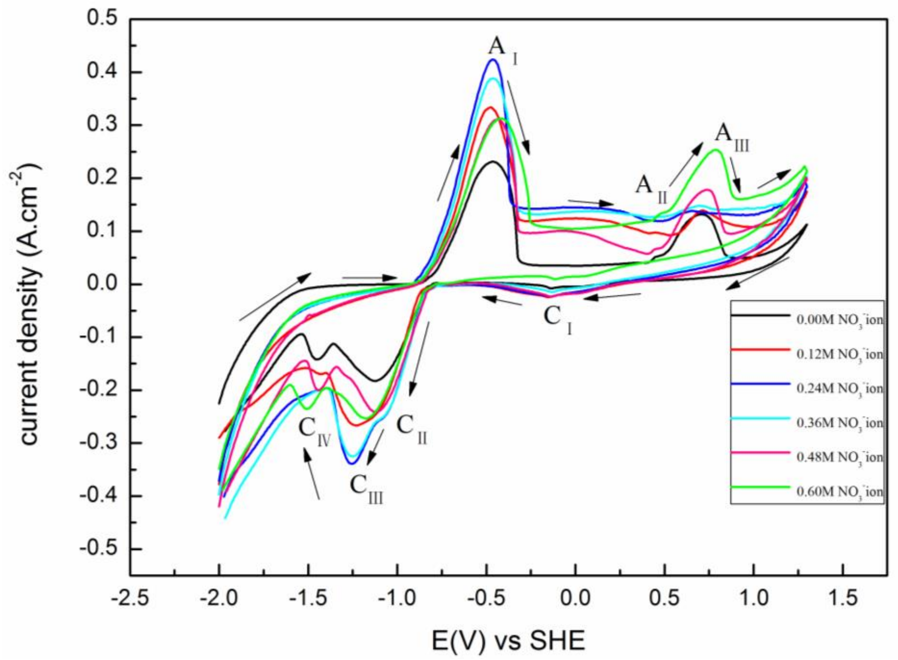

Figure. 2 Cyclic voltammogram of the Pb electrode in 4 M NaOH solution with different NO_3^- concentrations (scan rate, 50 mV/s).

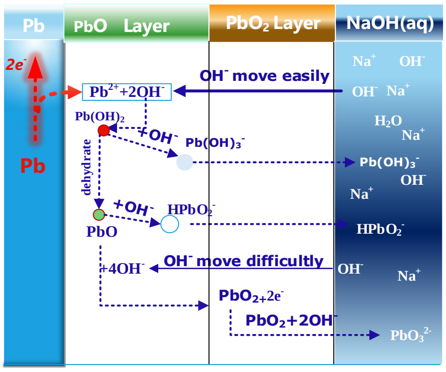

Figure 3. Mechanism for the formation and dissolution of PbO and PbO_2 on the surface of the lead electrode in NaOH solution.

However, when the external potential is more positive than the potential of $Pb(OH)_2$ formation, PbO film generates through a direct nucleation process that can be described by the following chemical reactions [20]:

$$PbOH_{ads} + OH^- = PbO_{ads}^- + H_2O \qquad (6)$$

$$PbO_{ads}^- = PbO + e^- \qquad (7)$$

Peaks A_{II} and A_{III} appearing at 0.48 V and 0.72 V, respectively, in Fig. 2 are assigned to the formation of Pb_3O_4 and PbO_2, respectively, according to the following equations [11]:

$$3PbO + 2OH^- = Pb_3O_4 + H_2O + 2e^- \qquad (8)$$
$$Pb_3O_4 + OH^- = 3PbO_2 + 2H_2O + 4e^- \qquad (9)$$

Thermodynamic analysis based on the φ-pH diagram of the Pb-N-Na-H_2O system indicates that PbO and PbO_2 partially dissolve as $HPbO_2^-$ and PbO_3^{2-} in strong alkaline solution. In the present investigation, the concentration of NaOH was controlled at 4 M, hence PbO and PbO_2 can chemically dissolve based on the following chemical reactions [11, 15]:

$$PbO + OH^- = HPbO_2^- \qquad (10)$$
$$PbO_2 + 2OH^- = PbO_3^{2-} + H_2O \qquad (11)$$

The cathodic branch of the cyclic voltammograms illustrates the reduction process of the oxidation products formed in the anodic oxidation process. Peak C_I corresponds to the reduction of external PbO_2 to Pb_3O_4. Peak C_{II} is assigned to the reduction of Pb_3O_4 to PbO. Peak C_{III} is due to the reduction of both PbO and PbO_2 to Pb. Peak C_{IV} seems to correspond to the formation of PbH_2 [9].

4.1.2 Effect of NO_3^- concentration on Peak A_I (PbO formation)

The effect of NO_3^- concentration on peak A_I at -0.46 V in the cyclic voltammograms is illustrated in Fig. 2. It is obvious that all current densities of Peak A_I in NaOH solution with NO_3^- added are higher than that of no NO_3^- addition. These results can be attributed to the effective oxidizing property of NO_3^-, which stimulates the oxidation of lead in NaOH solution.

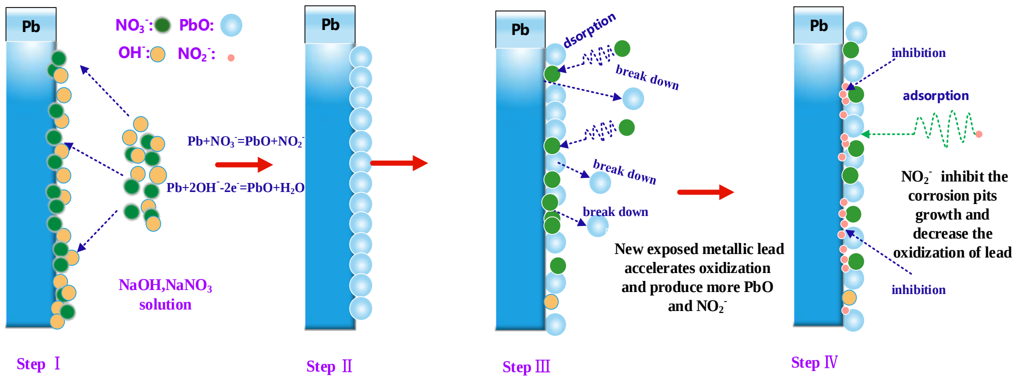

Figure. 4 Mechanism for NO_3^- influence on the formation of PbO on the surface of the lead electrode in NaOH solution.

NO_3^- shows a remarkable positive influence on the formation of PbO when its concentration range is 0.0~0.24 M. Over this range the density of peak A_I increases and reaches a maximum value when the NO_3^- concentration is 0.24 M. However, the positive effect of NO_3^- on PbO formation can be weakened slightly when the NO_3^- concentration is 0.36~0.60 M. Over this range the current density of peak A_I decreases gradually with increasing NO_3^- concentration. These results can be attributed to the influence of NO_3^- and NO_2^- on the formation of PbO. NO_3^- can be reduced to NO_2^- by metallic lead according to thermodynamic analysis. Fig. 4 displays the mechanism for the effect of NO_3^- and NO_2^- on PbO film formation.

When lead electrode is immersed in NaOH-$NaNO_3$ solution, competitive adsorption between OH^- and NO_3^- ions occurs on the surface of the lead electrode as shown in Step I, Fig. 4. This adsorption is essential for the first step of PbO film formation. Subsequently, metallic lead will be oxidized to PbO by OH^- and NO_3^-, which results in the formation of NO_2^- and PbO film as exhibited in Step II, Fig. 4.

The mechanism for the effect of NO_3^- on PbO film is shown in Step III, Fig. 4. NO_3^- was confirmed as a type of aggressive ion [14], such that the formed PbO film will suffer an attack from NO_3^-. NO_3^- can penetrate through the PbO film and break down PbO molecules, which directly leads to the exposure of fresh lead surface to the solution. Fresh lead surface contacts the bulk solution and produces more PbO and NO_2^- with increasing NO_3^- concentration. This speculation was confirmed by the variation tendency of peak A_I (formation of PbO) shown in Fig. 2.

Although NO_3^- can enhance the formation of PbO, excessive NO_3^- will weaken its positive effect. The mechanisms are illustrated by Step IV in Fig. 4. A previous study provided evidence that NO_2^-, the main reduction product of NO_3^-, was a type of inhibitor of lead corrosion [15]. The formation of PbO can be inhibited when NO_2^- ions are absorbed on the surface of the lead in the solution. As mentioned above, the oxide film can be broken by increasing NO_3^- concentration, which results in more fresh lead exposed to the solution as shown in Step III, Fig. 4. The increasing NO_3^- concentration can be reduced by fresh lead, producing more NO_2^- according to Equation (1). Therefore, the inhibitory effect of NO_2^- is more pronounced with the increase of NO_3^- concentration as shown in Fig. 2. Therefore**,** the current density of Peak A_I (formation of PbO) decreased gradually when NO_3^- concentration increased from 0.36 to 0.60 M.

Based on the analysis above, a conclusion can be drawn that when NO_3^- is added to the NaOH solution, two possible mechanisms will intervene in the formation of PbO on the lead electrode surface, one being the positive effect of NO_3^- and the other being the inhibitory effect of NO_2^- . NO_2^- is derived from NO_3^- reduction. Therefore, over-dosage or no NO_3^- addition is disadvantageous for the formation of PbO through peak A_I. An appropriate dosage of NO_3^- benefits the formation of PbO on the lead surface in NaOH solution. NO_3^- displays a positive effect on the formation of PbO and the yield of PbO increases obviously with NO_3^-concentration, from 0 M to 0.24 M. However, when the NO_3^- concentration range is 0.36~0.60 M, NO_3^- displays a negative effect on the formation of PbO. The yield of PbO decreases with increasing NO_3^- concentration because more NO_2^- can be obtained, which can inhibit the formation of PbO.

4.1.3 Effect of NO_3^- concentration on peak A_{III} (PbO_2 formation)

The effect of NO_3^- concentration on peak A_{III} (at 0.72 V, formation of PbO_2) is shown in Fig. 2. As seen in Fig. 2, the current density of peak A_{III} increased obviously when the concentration of NO_3^- increased from 0.0 to 0.60 M, which indicates that the addition of NO_3^- benefits the formation of PbO_2. The reoxidation of PbO and Pb_3O_4 can be suggested as the probable route of PbO_2 formation on the surface of lead. This possible mechanism is exhibited in Fig. 5.

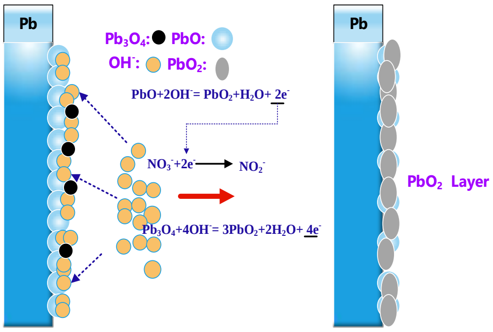

Figure 5. Mechanism for PbO_2 formation on the surface of lead in NaOH-$NaNO_3$ solution

Previous analysis indicates that when a lead electrode is immersed in NaOH-$NaNO_3$ solution PbO and Pb_3O_4 can be found on its surface. When the potential is more positive PbO and Pb_3O_4 can be oxidized to PbO_2 according to the reactions shown in equation (8) and (9).

The current density of PbO_2 formation increases slowly when the NO_3^- concentration increases from 0.12 to 0.24 M. However, the density of peak A_{III} (formation of PbO_2) increases rapidly when the NO_3^- concentration increases from 0.36 to 0.6 M. This can be ascribed to the powerful oxidizing properties of NO_3^- upon formation of PbO_2 in NaOH solution. The nitrogen atom in NO_3^- is in a high valence state when PbO and Pb_3O_4 lose electrons according to equation (8) and (9), and NO_3^- can play an electron acceptor role in the electrochemical reaction, which will promote the formation of PbO_2. Therefore, abundant NO_3^- ions are beneficial to the formation of PbO_2. This speculation is in accordance with the variation tendency of peak A_{III} (PbO_2 formation) shown in Fig. 2.

4.2. Electrochemical impedance spectroscopy (EIS) study

To investigate the anodic dissolution behavior of the lead electrode, electrochemical impedance spectroscopy (EIS) measurements were performed at -0.46 V (potential of peak A_I, the formation of PbO) and 0.72 V (potential of peak A_{III}, the formation of PbO_2) in 4 M NaOH solution with different concentrations of NO_3^-. The frequency range of EIS measurements is from 0.01 Hz to 100 kHz.

Electrode-equivalent circuits (EECs) with several electrical circuit elements were employed to model the anodic dissolution characteristics of lead in NaOH-$NaNO_3$ solution. The EECs used to fit experimental data are shown in Fig. 6(a) and Fig. 6(b). It is seen that $R_s(Q_1(R_{ct}W))(C_fR_f)$ is suitable for the EIS spectra obtained at the potential of peak A_I(-0.46 V). $R_s(Q_2R_{ct})$ is better for fitting the EIS spectra obtained at the potential of peak A_{III} (0.72 V). The parameters contained in the EECs are as follows: R_s, R_{ct}, W, C_f, R_f, Q_1, Q_2. R_s stands for the resistance of the solution, R_{ct} corresponds to the charge transfer resistance; W is the Warburg impedance associated with the diffusion of reactants or product species; C_f is the capacitance of oxidation film formed on the surface of the lead electrode in the NaOH-$NaNO_3$ solution and R_f is the resistance of lead oxidation film [21].

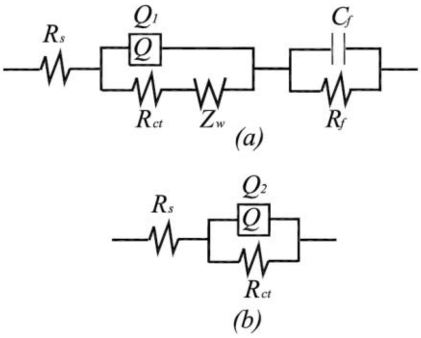

Figure 6. Electrode-equivalent circuits (EECs) for fitting EIS spectra obtained at fixed potentials in NaOH-$NaNO_3$ solution

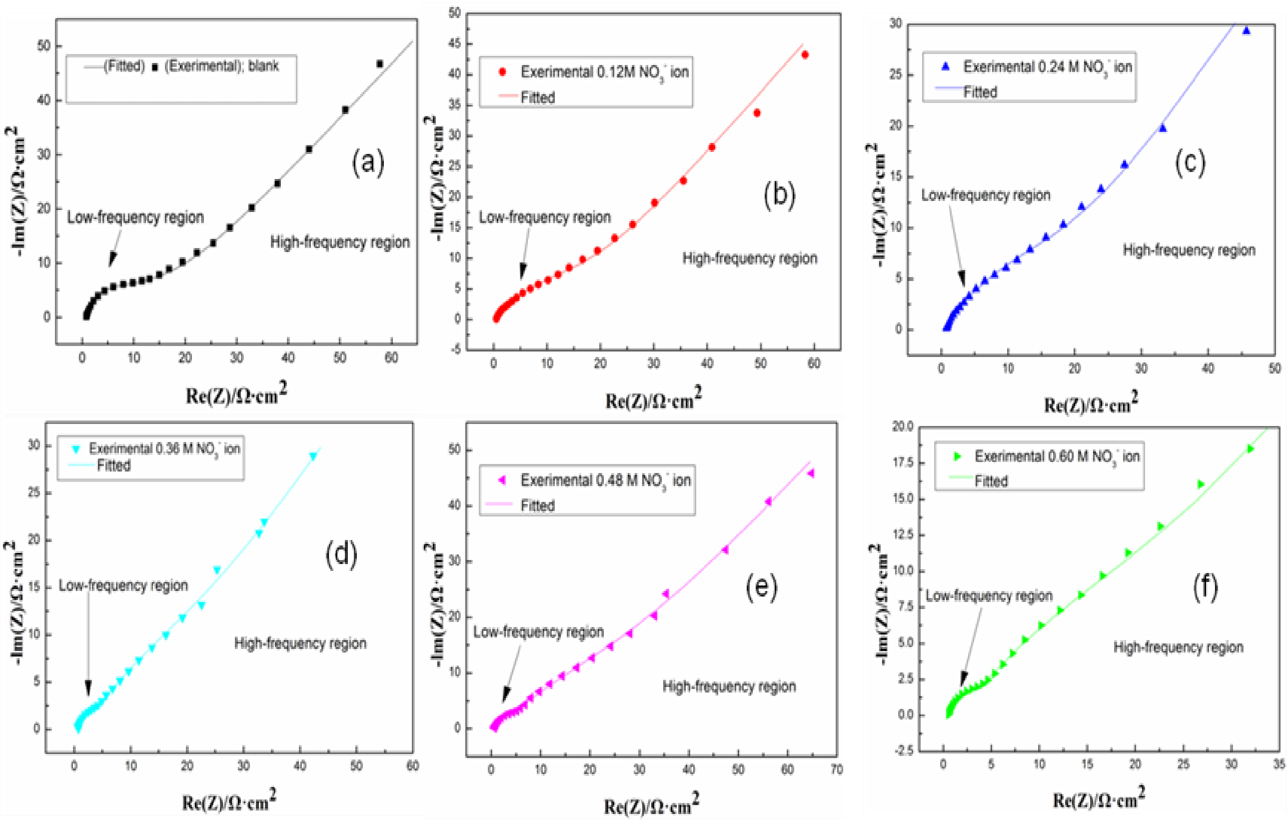

Figure 7. Nyquist plots of lead in 4 M NaOH solution with different NO_3^- concentrations at -0.46 V

Q_1 and Q_2 represent the constant phase element (CPE), which is widely used to model the impedance of complex real systems. The impedance of CPE can be defined by the following equation:

$$Z_{CPE} = [Y_0 (j\omega)^n]^{-1} \qquad (12)$$

where Y_0 is the modulus, ω is the angular frequency (in rad/s), j is an imaginary number and n is the exponent, which is an adjustable parameter ranging from 0 to 1. Different values of n have different physical significance to the constant phase element: when n equals 0, 0.5, and 1 the CPE corresponds to a resistance, Warburg impedance, and capacitance, respectively [22-23].

EIS results at -0.46 V (value of peak A_I) were presented as a Nyquist plot in Fig. 7. The best fitting parameters of the EIS spectra obtained at -0.46 V (value of peak A_I) have been simulated by Zsimp Win software. The results are shown in Table 1.

Table 1. EIS data simulations for a lead electrode in 4 M NaOH solution with different NO_3^- concentrations at -0.46 V; fit with EEC (a)

NO_3^- ion (M)	0.00	0.12	0.24	0.36	0.48	0.60
R_s (Ω cm^2)	0.7282	0.4476	0.6839	0.5548	0.4475	0.4621
Error%	2.01	1.56	1.23	1.44	2.86	3.02
R_{ct} (Ω cm^2)	16.04	20.19	24.13	45.05	44.82	42.76
Error%	1.15	1.88	1.04	1.63	1.58	1.87
$Q(\Omega^{-1}\ cm^{-2}\ s^{-n})$	2.279×10^{-3}	2.786×10^{-3}	4.308×10^{-3}	9.492×10^{-3}	6.574×10^{-3}	1.5350×10^{-2}
Error%	1.32	1.50	1.26	1.24	1.68	2.05
n	0.6482	0.6295	0.5753	0.5092	0.5336	0.4916
Error%	0.59	0.25	0.38	0.97	0.81	0.72
Z_W(Ω cm^2)	0.01634	0.01829	0.02088	0.01644	0.01353	0.01326
Error%	2.21	1.65	2.43	2.02	2.65	1.98
C_f(F cm^{-2})	2.38×10^{-4}	2.97×10^{-4}	6.02×10^{-4}	1.77×10^{-4}	1.48×10^{-4}	2.13×10^{-4}
Error%	1.13	1.05	0.89	1.50	1.06	1.28
R_f (Ω cm^2)	4.0070	0.8588	0.5592	1.3690	1.8410	1.3810
Error%	2.78	1.55	1.37	2.94	2.11	1.05

The EIS curves in Fig. 7 exhibit semicircles that are not well defined in high frequency regions and are approximately linear in low frequency regions. The semicircle at high frequencies is attributed to the charge transfer process whereas the approximately straight line at low frequencies can be considered the effect of the oxidation layer on mass transportation [24].

Table 1 shows that the value of charge transfer resistance (R_{ct}) increases with the NO_3^- concentration increase from 0 to 0.36 M. When the concentration of NO_3^- exceeds 0.36 M the value of R_{ct} begins to decrease gradually. This behavior can be explained as follows: when NO_3^- is absent from the solution, the lead electrode in NaOH solution can be considered an active dissolution and the electric charge can easily transfer between electrode surface and bulk solution with little resistance, hence transfer resistance R_{ct} is at a minimum. However, when the NO_3^- concentration increases from 0.12 to 0.36 M in NaOH solution, the transfer resistance R_{ct} increases obviously. This trend can be attributed to the formation of an oxidation layer. According to previous analysis, when the NO_3^- concentration range is 0～0.36 M, NO_3^- benefits the formation of PbO. The main products on the surface of the lead electrode are PbO and a trace of Pb_3O_4. The mixture of PbO and Pb_3O_4 on the lead surface can be speculated as lead non-stoichiometric oxide compounds (PbO_x), and the conductivity of PbO_x is related to the value of x. PbO_x could be either a conductor (x close to 2) or an insulator (x close to 1) [6].

When the NO_3^- concentration increases from 0 to 0.36 M the yield of PbO increases and most of the oxidative layer is close to PbO. PbO_x can be an insulator (when x is close to 1) so the oxidative layer can be considered a poor conductor, which causes the high resistance to charge transfer. As a result, the value of R_{ct} increases obviously when the NO_3^- concentration increases from 0 to 0.36 M.

In contrast, when the NO_3^- concentration exceeds 0.36 M, the formed PbO and Pb_3O_4 on the lead electrode surface will be damaged by NO_3^- and the renascence of PbO will be inhibited by NO_2^-. Therefore, the yield of PbO will decrease gradually, and PbO_x on the lead electrode surface can be considered a conductor [6, 25], hence the conductivity of the oxidative layer will be gradually improved and its resistance to charge transfer will decrease gradually as shown in Table 1**.**

In addition, Fig. 7 shows that all plots are approximately linear at low frequencies, which corresponds to Warburg type impedance (Z_w). Warburg responses observed in this case are due to the formation of PbO (Pb_3O_4) films on the electrode surface, which shows a shielding effect on mass transport of reactants and products [24].

The variation tendency of Z_W shown in Table 1 exhibits good agreement with the variation tendency of PbO formation at the potential of peak A_I (-0.46 V) shown in Fig. 2. When the NO_3^- ion concentration is 0～0.24 M, Z_W increases gradually from 0.01634 Ω cm^2 to 0.02088 Ω cm^2. This phenomenon might be attributed to the beneficial effect of NO_3^- on the formation of PbO. When NO_3^- is absent from the solution Z_W is small due to a small quantity of PbO (Pb_3O_4) films formed on the electrode surface. Therefore, the resistance to mass transport among the lead surface, NO_3^- and OH^- in bulk solution is low. However, when the concentration of NO_3^- increases from 0.12 to 0.24 M, PbO (Pb_3O_4) films on the lead electrode become thicker and the resistance of mass transportation (Z_W) increases gradually [24]. Z_W reaches the maximum value when the NO_3^- concentration is 0.24 M, which is the optimum NO_3^- concentration for the formation of PbO.

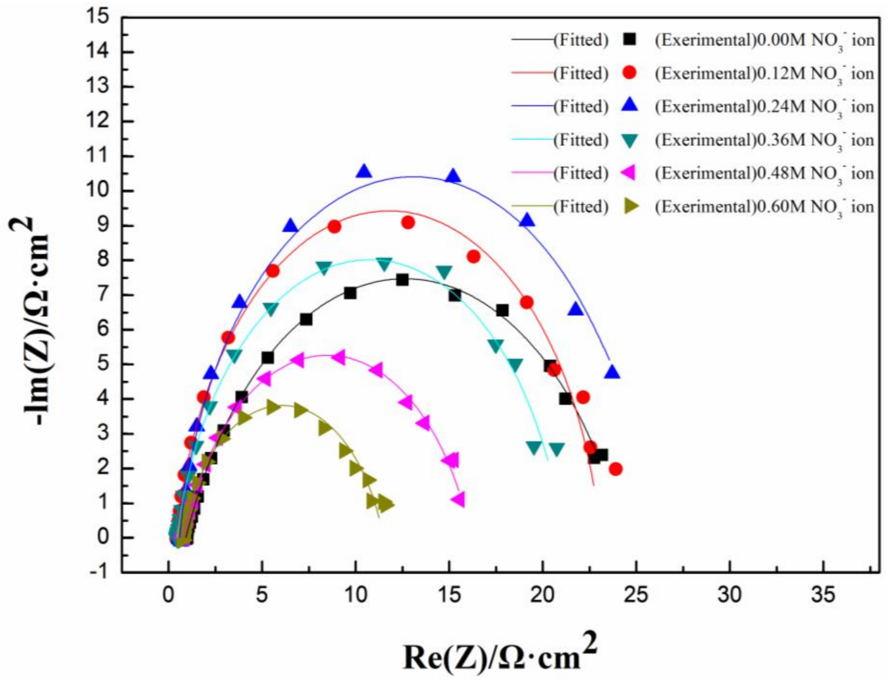

Figure 8. Nyquist plots of lead in 4 M NaOH solution with different NO_3^- concentrations at 0.72 V

Table 2. EIS data simulations for a lead electrode in 4 M NaOH solution with different NO_3^- ion concentrations at 0.72 V; fit with EEC (b)

NO_3^- ion (M)	0.00	0.12	0.24	0.36	0.48	0.60
Rs (Ω cm^2)	0.9311	0.4483	0.5926	0.4527	0.8037	0.7004
Error%	0.85	1.67	1.41	1.29	1.03	1.23
Rct (Ω cm^2)	25.000	22.620	20.620	16.040	15.360	10.770
Error%	2.96	5.34	4.13	4.01	4.04	5.38
$Q(\Omega^{-1}\ cm^{-2}\ s^{-n})$	1.419×10^{-2}	4.627×10^{-3}	7.544×10^{-3}	8.573×10^{-3}	9.369×10^{-3}	7.777×10^{-3}
Error%	0.79	1.16	1.202	0.984	1.06	1.29
n	0.7316	0.9003	0.8998	0.8547	0.8037	0.7949
Error%	1.52	2.60	3.45	2.34	1.87	1.95

When the NO_3^- concentration is over 0.24 M, Z_W decreases gradually because the yield of PbO decreases under such conditions. The decreasing amount of PbO is ascribed to the destructive effect of NO_3^- on the formed PbO film and the inhibitory effect of NO_2^- on the renascence of PbO film on the lead electrode. The decrease in the amount of PbO film will reduce the resistance to mass transport among the lead surface, NO_3^- and OH^- in bulk solution. Consequently, the value of Z_W decreases gradually when the NO_3^- concentration increases from 0.36 to 0.60 M.

The selected potential of 0.72 V (value of peak A_{III}) is presented as a Nyquist plot in Fig. 8. The best fitting parameters of the EIS spectra obtained at 0.72 V were simulated by Zsimp Win software. The fitting EEC in Fig. 6(b) gave satisfactory results and the best fitting parameters are listed in Table 2.

The semicircles in the high frequency region of the EIS spectra in Fig. 8 indicate that the charge transfer process plays a central role during PbO_2 formation. Table 2 shows that the value of charge transfer resistance (R_{ct}) decreases gradually when NO_3^- concentration increases from 0.00 M to 0.60 M. This variation tendency is due to changes in the composition of the oxidation film on the surface of the lead electrode. As shown in Fig. 5, the formation of PbO_2 is mainly caused by the reoxidation of PbO and Pb_3O_4. When abundant NO_3^- was added to the solution, the formation of PbO_2 was enhanced. With more PbO_2 generated, the conductivity of the lead surface is obviously improved because PbO_2 is a good conductor [6, 26]. Therefore, the charge transfer resistance (R_{ct}) decreases gradually when the concentration of NO_3^- increases from 0.0 to 0.60 M, as shown in Table 2.

4.3. Surface analysis

4.3.1 Scanning Electron Microscope analysis

To investigate the effect of NO_3^- on the anodic behavior of lead in NaOH-$NaNO_3$ solution, a scanning electron microscope (SEM) analysis was conducted. The scanning electron micrographs are shown in Fig. 9. Fig. 9(a) is related to the SEM image of a fresh polished lead electrode, Fig. 9(b) and Fig. 9(c) are assigned to the SEM images of the lead surface after potentiostatic polarization for 20 min in NaOH-$NaNO_3$ solution at -0.46 V (potential of peak $A_{I,}$ the formation of PbO). Fig. 9(d) and Fig. 9

(e) are related to the surface morphology of the lead surface after potentiostatic polarization for 20 min in NaOH-NaNO$_3$ solution at 0.72 V (potential of peak A_{III}, the formation of PbO$_2$).

The effects of NO$_3^-$ addition on surface microstructures can be clearly observed based on Fig. 9. It is seen in Fig. 9(b) and Fig. 9(c) that when NO$_3^-$ is added to the solution the surface of the electrode appears more porous. Similarly, the surface of the lead shown in Fig. 9(e) also seems more porous than that shown in Fig. 9(d).

The surface morphology confirmed that NO$_3^-$ in NaOH solution can break down the formed oxidization film on the surface of the lead electrode and make the surface porous. The porous surface makes the oxidization film loose and chemically reactive. Corrosion holes and cracks on the lead electrode surface shown in Fig. 9(c) and Fig. 9(e) confirm the aggressive effect of NO$_3^-$ on the surface of the lead electrode.

As analyzed above, the addition of NO$_3^-$ ion causes significant change in the surface morphology of the lead electrode. A suitable NO$_3^-$ concentration makes the electrode surface become more chemically reactive, which benefits the formation of lead oxides on the lead electrode surface. This variation tendency is in accordance with the change trend of the potential of peak A_I and A_{III} shown in the cyclic voltammogram, Fig. 2. Fig. 2 shows that all current densities of peaks A_I and A_{III} in NaOH solution are higher with added NO$_3^-$ than without, which indicates that the addition of NO$_3^-$ will improve the anodic oxidation reactions.

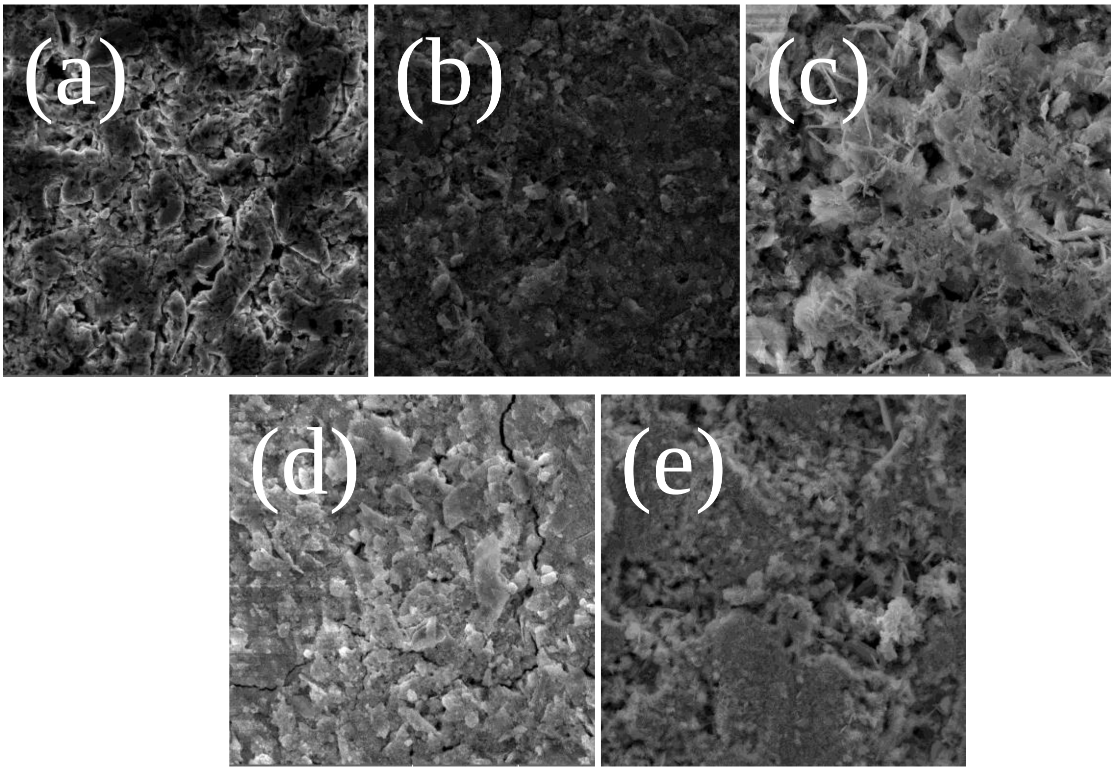

Figure 9. Surface morphologies of the lead electrode after potentiostatic polarization at a fixed potential for 20 min in 4 M NaOH solution with different NO$_3^-$ concentrations: (a) pure surface of lead electrode; (b) at a fixed potential of -0.46 V in 4 M NaOH; (c) at a fixed potential of-0.46 V in 4 M NaOH with 0.24 M NO$_3^-$ added; (d) at a fixed potential of 0.72 V in 4 M NaOH; (e) at a fixed potential of 0.72 V in 4 M NaOH with 0.6 M NO$_3^-$ added.

The cyclic voltammetry results and SEM analysis indicate that the addition of NO_3^- can accelerate the formation of lead oxides on the surface of the lead electrode in NaOH solution.

4.3.2 X-ray photoelectron spectroscopy analysis

To investigate the chemical composition of the lead electrode surface after potentiostatic polarization for 20 min in NaOH-$NaNO_3$ solution at a fixed potential, X-ray photoelectron spectroscopy (XPS) measurements were performed and the results are shown in Fig. 10.

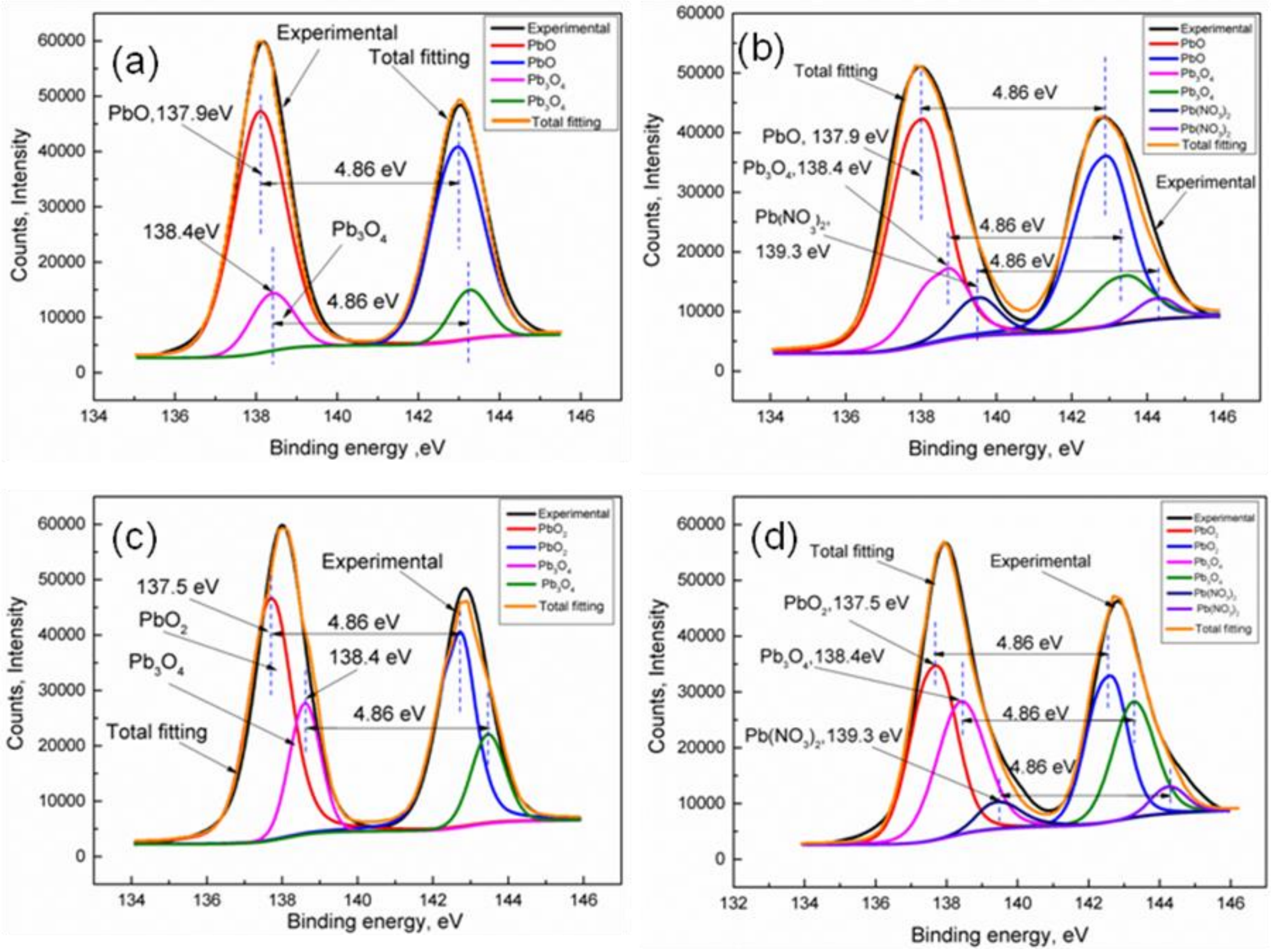

Figure 10. Pb4f7/2 and Pb4f5/2 spectra for the lead electrode surface obtained after potentiostatic polarization at a fixed potential for 20 min in 4 M NaOH solution with different NO_3^- concentrations: (a) at a fixed potential of -0.46 V in 4 M NaOH; (b) at a fixed potential of -0.46 V in 4 M NaOH with 0.24 M NO_3^- added; (c) at a fixed potential of 0.72 V in 4 M NaOH; (d) at a fixed potential of 0.72 V in 4 M NaOH with 0.6 M NO_3^- added.

The Pb4f7/2 and Pb4f5/2 spectra were investigated to determine the chemical composition on the surface of the lead electrode. The accuracy of the binding energies is ±0.1 eV. The C1s peak at 284.8 eV, a contamination carbon, is used as a reference for all spectra.

The Pb4f spectra shown in Fig. 10 indicate that element Pb on the surface of the lead electrode is not present in metallic form according to its peak position. The peak position of metallic Pb in Pb4f is 136.9 eV [27] whereas the Pb4f7/2 and Pb4f5/2 peak positions shown in Fig. 10 are above 136.9 eV. This result indicates that Pb on the surface of lead electrodes has lost electrons and the binding energy becomes more positive. From its position, lead is judged to be in a metal-oxide form and to have more than one chemical state.

XPS spectra of the lead surface after potentiostatic polarization in NaOH-$NaNO_3$ solution at -0.46 V are shown in Fig. 10(a) and Fig. 10(b), respectively. XPS spectra of the lead surface after potentiostatic polarization at 0.72 V are shown in Fig. 10(c) and Fig. 10(d). As shown in Fig. 10, the peak at 137.9 eV is attributed to PbO [28], the peak at 138.4 eV corresponds to Pb_3O_4 [29], and the peak at 137.5 eV corresponds to PbO_2 [27].

The peaks at 139.3 eV shown in Fig. 10(b) and Fig. 10(d) are assigned to $Pb(NO_3)_2$ [27]. According to Fig. 10(c) and Fig. 10(d), PbO_2 is the main chemical component on the lead electrode surface after potentiostatic polarization at a potential of 0.72 V in NaOH-$NaNO_3$ solution.

As illustrated above, the main chemical component of the lead electrode surface after potentiostatic polarization at -0.46 V (the potential of peak A_I, shown in the cyclic voltammogram in Fig. 2) is PbO. The main chemical component of the lead electrode surface after potentiostatic polarization at 0.72 V (the potential of peak A_{III}, shown in the cyclic voltammogram in Fig. 2) is PbO_2.

The XPS results exhibit a good accordance with the cyclic voltammetry analysis: when NO_3^- is absence from NaOH solution, the main chemical component on the lead surface is PbO and PbO_2 after potentiostatic polarization at -0.46 V and 0.72 V, respectively. As an intermediate oxide, Pb_3O_4 can be detected in all samples. This phenomenon is in good accordance with the cyclic voltammogram shown in Fig. 2. The peak of Pb_3O_4 (peak A_{II}) can be observed on the cyclic voltammetry curves shown in Fig. 2. $Pb(NO_3)_2$ can also be found on the surface of the lead electrode when NO_3^- is adopted. The formation of $Pb(NO_3)_2$ is due to the adsorptive NO_3^- combined with Pb^{2+} on the lead surface. The percent compositions of the lead metal-oxide states on the lead surface obtained under different conditions are shown in Table 3.

Table 3. The composition of lead metal-oxides states on the surface of lead obtained under different conditions.

Fig10.No.	NO_3^-ion (M)	potential (V)	PbO (%)	Pb_3O_4(%)	PbO_2(%)	$Pb(NO_3)_2$(%)
(a)	0.00	-0.46	89.72	10.28	-	-
(b)	0.24	-0.46	84.64	12.83	-	2.53
(c)	0.00	0.72	-	41.43	58.57	-
(d)	0.60	0.72	-	32.66	64.19	3.15

5. CONCLUSION

In this study, the effect of NO_3^- concentration on lead anodic electrochemical behavior in NaOH solution was investigated using cyclic voltammetry (CV) and electrochemical impedance spectroscopy (EIS). The surface characteristics of lead after potentiostatic polarization were examined by scanning electron microscopy (SEM) and X-ray photoelectron spectroscopy (XPS). NO_3^- displays a positive effect on the formation of PbO from 0.0～0.24 M and a negative influence from 0.36～0.60 M. The positive influence of NO_3^- is attributed to the strong oxidizing property and the aggressive effect of NO_3^-, whereas the negative influence of NO_3^- is ascribed to the inhibitory effect of NO_2^-, which originates from the reduction of NO_3^- by lead. A high NO_3^- concentration is good for the formation of PbO_2 at 0.72 V.

Mechanisms for the influence of NO_3^- on the formation of PbO and PbO_2 on the surface of lead have been proposed. The lead anodic electrochemical behavior in NaOH-$NaNO_3$ solution has been successfully illustrated based on the mechanisms. EIS analysis indicates that the variation tendency of charge transfer resistance (R_{ct}) is in accordance with the effect of NO_3^- concentration on the lead anodic behavior in NaOH-$NaNO_3$ solution. SEM observation confirmed the aggressive effect of NO_3^- on the formed films on the lead surface. XPS results indicate that the chemical components of the lead electrode surface in NaOH-$NaNO_3$ solution obtained at different potentials are PbO, Pb_3O_4, PbO_2 and $Pb(NO_3)_2$, which agrees with the results of cyclic voltammetry.

ACKNOWLEDGMENTS
The authors gratefully acknowledge the financial support of the National Natural Science Foundation of China (Grant No. 51564031) and the financial support of the cooperation between school and enterprise of China (Grant No. 0201352042)

References

1. N. Hirai and Y. Yamamoto, *J. Power Sources* 293 (2015) 1073.
2. W. Zhang, C. Q. Tu, Y. F. Chen, W. Y. Li and G. Houlachi, *J. Mater. Eng. Perform*. 22 (2013) 1672.
3. N. Hirai, D. Tabayashi, M. Shiota and T. Tanaka, *J. Power Sources* 133 (2004) 32.
4. D. Pletcher, H .Zhou, G. Kear, C.T.J. Low, F.C. Walsh and R .G. A. Wills, *J. Power Sources* 180 (2008) 621.
5. Z. Wu, D. B. Dreisinger, H. Urch and S. Fassbender, *Hydrometallurgy* 142 (2014) 23.
6. A .Oury, A. Kirchev, Y. Bultel and E. Chainet, *Electrochim. Acta* 71 (2012) 140.
7. X. Zhu, L. Li, X.Sun, D.Yang, L. Gao, J. Liu, R.V. Kumar and J. Yang, *Hydrometallurgy* 117 (2012) 24.
8. B. Zhang, J. Zhong, B. Zhang and Z. Cheng, *J. Power Sources* 196 (2011) 5719.
9. E. F. El-Sherbini and S. S. A. E. Rehim, *Mater. Chem. Phys*. 88 (2004) 17.
10. M. M. El-Naggar, *J. Power Sources* 126 (2004) 207.
11. E.E. Abdelaal，S.Abdel Wanees and A.abdeaal, *J. Mater. Sci*.28 (1993) 2607.
12. M. A. Amin, and S. S. A. Rehim, *Electrochim. Acta* 49 (2004) 2415.
13. A. A. Montaser, P. Veluchamy and H. Minoura, *J. Electroanal. Chem*. 419 (1996) 47.
14. S. S. Abd EL- Rehim.and N. F. Mohamed, *Corros. Sci*. 11 (1998) 1883.
15. M. Uchida and A. Okuwaki, *Corros. Sci*. 41 (1999) 1977.
16. M. Uchida and A. Okuwaki, *Hydrometallurgy* 49 (1998) 297.
17. Y.N. Vodyanitskii and V.G. Mineev, *Eurasian Soil Sci.* 48(2015)139.
18. M. Pourbaix, *Atlas of Electrochemical Equilibria in Aqueous Solutions*, Pergamon, Oxford(1966).
19. V.I. Briss and M. T. Shevalier, *J. Electrochem. Soc*.134 (1987) 804.
20. V.I. Briss and M. T. Shevalier, *J. Electrochem. Soc*.137 (1990) 2643.
21. Y. Pan, Y. Wen, L. Xue, X. Guo and H. Yang, *J. Phys. Chem*. C 116 (2012) 3532.

22. S. Fajardo, D. M. Bastidas, M. Criado, M. Criado and J. M. Bastidas, *Electrochim. Acta* 129 (2014) 160.
23. H. Luo, C. F. Dong, X. G. Li and K. Xiao, *Electrochim. Acta* 64 (2012) 211.
24. M. Mouanga and P. Bercot, *Corros. Sci*. 52 (2010) 3993.
25. W. Cai, Y. Wan, H. Liu and W. Zhou, *J. Electroanal. Chem*. 387 (1995) 95.
26. J. Pohl and G. Schlechtriemen, *J. Appl. Electrochem*. 14 (1984) 521.
27. J. F. Moulder, W. F. Stickle, P. E. Sobol, and K. D. Bomben, *Handbook of X- Ray Photoelectron Spectroscopy*, Physical Electronic, Inc., Minnesota, USA(1995)
28. C. D. Wanger, W. M. Riggs, L. E. Davis and J. F. Moulder, *Handbook of X-Ray Photoelectron Spectroscopy*, Perkin-Elmer Corporation Physical Electronics Division, Minnesota, USA(1979)
29. K. S. Kim, T. J. O'Leary and N. Winograd, *Anal.Chem*. 45 (1973) 2215.